



# Silica-supported chromia-titania catalysts for selective formation of lactic acid from a triose in water

Atsushi Takagaki<sup>\*,1</sup>, Hiroshi Goto, Ryuji Kikuchi, S. Ted Oyama

Department of Chemical System Engineering, School of Engineering, The University of Tokyo, 7-3-1 Hongo, Bunkyo-ku, Tokyo, 113-8656, Japan

## ARTICLE INFO

### Keywords:

Lactic acid  
Dihydroxyacetone  
Brønsted acid  
Lewis acid  
Supported metal oxide catalyst

## ABSTRACT

A variety of silica-supported metal oxide catalysts were prepared by the incipient wetness impregnation method and were used for the conversion of dihydroxyacetone to lactic acid. A titanium oxide catalyst with Brønsted acid sites was selective to an intermediate, pyruvaldehyde and a chromium oxide catalyst with Lewis acid sites was selective to lactic acid. The co-impregnation of chromium- and titanium oxides with different ratios accelerated the reaction rate and improved the lactic acid yield up to 80% at 130 °C. Pyridine-adsorbed Fourier-transform infrared spectroscopy indicated that the silica-supported mixed oxides had both Brønsted acid and Lewis acid sites and the trend of the Lewis/Brønsted ratio was close to that of selectivity to lactic acid. Diffuse reflectance UV–vis spectroscopy showed that the silica-supported chromia-titania catalyst composed of isolated Cr and Ti species in tetrahedral coordination. Kinetic analysis revealed that the two critical rate constants, pyruvaldehyde formation and lactic acid formation, for the chromia-titania catalyst were much higher than those of the titania and chromia catalysts.

## 1. Introduction

Chemical production from biomass had attracted much attention because of potential to replace existing petroleum-based industries and to reduce carbon dioxide emissions. Lactic acid is one representative of sugar-derived chemicals and is used as a raw material for biodegradable plastics and solvents. The current industrial production method of lactic acid is an anaerobic fermentation of glucose and sucrose using microorganisms. This process, however, has several drawbacks such as low production rate and the use of a stoichiometric amount of base for neutralization to keep the preferable pH level for microorganism. Hence, the development of catalytic routes for conversion of sugars to lactic acid is needed [1].

One of the essential reaction steps for lactic acid (LA) production is the conversion of triose sugars, dihydroxyacetone (DHA) and glyceraldehyde (GLA) to LA (Scheme 1). Both trioses can be obtained by retroaldol condensation of glucose [2] which is derived from cellulose, or oxidation of glycerol which is the main byproduct of biodiesel from triglycerides [3]. This reaction step proceeds through dehydration of DHA or GLA to pyruvaldehyde (PA), an intermediate, followed by hydration and hydride shift. The first step, DHA or GLA dehydration followed by rearrangement, is catalyzed by both Brønsted and Lewis acid [4–6]. PA is further transformed into LA catalyzed by Lewis acids.

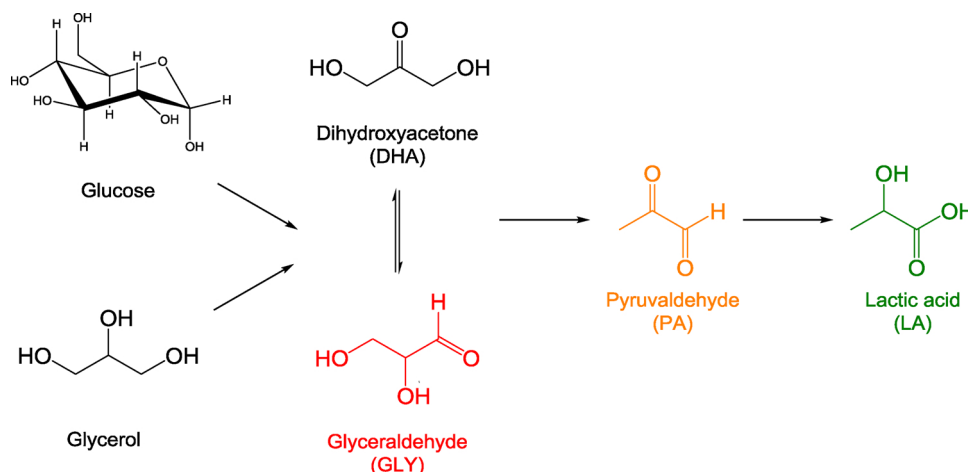
A large amount of research for the catalytic production of lactic acid or alkyl lactate by both homogeneous and heterogeneous catalysts has been conducted during recent years. As homogeneous catalysts, Al<sup>3+</sup> and Cr<sup>3+</sup> Lewis acids were found to be active in DHA transformation into LA in aqueous media [6]. As heterogeneous catalysts, representative catalysts are zeolites [7–9], especially Sn incorporating zeolites [3,10]. The Sn-β zeolite exhibited almost 100% methyl lactate yield for DHA transformation and 40% yield for glucose transformation in methanol media. There are several other Sn incorporating silicate catalysts, using mesoporous silica [11] or a hybrid material composed of Sn-Si-MCM-41 and graphite-like carbon [12]. These catalysts have both Lewis acid sites and Brønsted acid sites. The combination of these two kinds of acid sites was also responsible for the high activity of bulk-type catalysts such as tin phosphate [13,14] and a niobium oxide with a deformed orthorhombic structure [15].

In this study, a variety of silica-supported metal oxide catalysts were prepared and were used for the transformation of DHA to LA. The synthesis of the supported catalysts was facile and atom-efficient which contrasts with those of Sn-β zeolite and bulk materials because the former needs long synthesis time (days) and the latter can function only on the surface. It was found that the supported titanium oxide and chromium oxide were active for the transformation of DHA. The combination of the two metal oxides which have both Brønsted acid and

\* Corresponding author.

E-mail address: [atakagak@cstf.kyushu-u.ac.jp](mailto:atakagak@cstf.kyushu-u.ac.jp) (A. Takagaki).

<sup>1</sup> Present address: Department of Applied Chemistry, Faculty of Engineering, Kyushu University, 744 Motoooka, Nishi-ku, Fukuoka, 819-0395, Japan.



Scheme 1. Reaction pathways for lactic acid formation.

Lewis acid sites accelerated both the rates of DHA conversion and LA formation resulting in LA yield up to 80%.

## 2. Experimental

### 2.1. Chemicals

Dihydroxyacetone dimer (98%, Wako), DL-glyceraldehyde (97%, Wako), pyruvaldehyde (40% solution in water, Sigma-Aldrich) and lactic acid (85–92%, Kanto Chemical) were used for the reactions and the analysis. A fumed silica, Cab-o-Sil EH5 (Cabot) was used as inert support. Metal salts were purchased from Wako. Used as precursors were  $\text{Al}(\text{NO}_3)_3 \cdot 9\text{H}_2\text{O}$ ,  $\text{Ti}(\text{SO}_4)_2$  30% solution in water,  $\text{Cr}(\text{NO}_3)_3 \cdot 9\text{H}_2\text{O}$ ,  $\text{Mn}(\text{NO}_3)_2 \cdot 6\text{H}_2\text{O}$ ,  $\text{Fe}(\text{NO}_3)_3 \cdot 9\text{H}_2\text{O}$ ,  $\text{Ni}(\text{NO}_3)_2 \cdot 6\text{H}_2\text{O}$ ,  $\text{Zn}(\text{NO}_3)_2 \cdot 6\text{H}_2\text{O}$ ,  $\text{Ga}(\text{NO}_3)_3 \cdot n\text{H}_2\text{O}$ ,  $\text{In}(\text{NO}_3)_3 \cdot 3\text{H}_2\text{O}$ ,  $\text{SnCl}_4$ ,  $\text{WCl}_4$ , and  $\text{Pb}(\text{NO}_3)_2$ .

### 2.2. Catalysts preparation

The silica-supported metal oxide catalysts were prepared by incipient wetness impregnation and subsequent calcination. Typically, a quantity of 1 mmol of metal salts dissolved in distilled water was impregnated dropwise on 1 g of a fumed silica (Cab-o-sil, EH5) followed by calcination in air at 500 °C for 3 h. The catalysts used were named with their metal loading amount. For example, Cr(1.0)/SiO<sub>2</sub> indicates that 1.0 mmol of chromium was impregnated on 1.0 g of silica support.

### 2.3. Characterization

The prepared catalysts were characterized by X-ray diffraction (XRD; RINT-2700, Rigaku), and diffuse reflectance UV–vis spectroscopy (DR UV–vis; V-670, JASCO). The types of acid sites were distinguished using pyridine adsorbed Fourier-transform infrared spectroscopy (FTIR; FT/IR 6100, JASCO) equipped with a mercury cadmium telluride (MCT) detector with a resolution of 4 cm<sup>-1</sup>. The sample was pressed into disks with a radius of 1.0 cm at 15 MPa and a weight of 30 mg and then pretreated in the cell at 150 °C in a vacuum for 1 h. The sample was cooled to 100 °C, and a spectrum was measured. Pyridine gas was introduced to the cell, and the sample was contacted with pyridine for 30 min at 5 Torr. After pyridine was pumped off for 30 min, a spectrum of pyridine adsorbed sample was recorded. A difference spectrum was obtained by subtracting the spectrum of the dehydrated sample from the spectrum of the adsorbed sample. The amounts of Brønsted acid sites and Lewis acid sites were determined on the basis of the integral absorbance of the characteristic bands at 1545 cm<sup>-1</sup> for Brønsted acid sites and 1450 cm<sup>-1</sup> for Lewis acid sites by using integrated molar extinction coefficients, 1.67 cm μmol<sup>-1</sup> for Brønsted acid sites and

2.22 cm μmol<sup>-1</sup> for Lewis acid sites. [16]

### 2.4. Catalytic tests

A quantity of 0.55 mmol (50 mg) of dihydroxyacetone and 50 mg of silica-supported metal oxide catalysts was put into 3 mL water in a reactor vessel. The reactor vessel was heated at 130 °C for 3 h in an oil bath under stirring. After the reaction, reactant mixture was analyzed by high-performance liquid chromatography (HPLC; LC-2000 plus, JASCO) equipped with a differential refractive index detector (RI-2031 plus, JASCO) with Aminex HPX-87H column (flow rate: 0.5 mL min<sup>-1</sup>, eluent: 10 mM H<sub>2</sub>SO<sub>4</sub>).

## 3. Results and discussions

### 3.1. Screening of silica-supported metal oxide catalysts

The catalytic activities of a variety of supported metal oxides for lactic acid formation were surveyed. Twelve metal oxides, Al, Ti, Cr, Mn, Fe, Ni, Zn, Ga, In, Sn, W, and Pb oxides were chosen for the screening test because these metal salts were reported to be effective homogeneous catalysts to produce lactic acid from cellulose in aqueous media [17]. The amount of loading of metals was set to 1.0 mmol g<sup>-1</sup>. Fig. 1 shows the XRD patterns of silica-supported metal oxide catalysts. A broad peak around 20° was observed for all samples, which was attributed to amorphous silica. The samples of Cr, Mn, Fe, Ni, In, Sn, and W oxides had diffraction peaks attributable to corresponding metal oxides for each species. In contrast, the samples of Al, Ti, Zn, Ga, and Pb oxides showed no apparent peaks, indicating that these metal species were highly dispersed on silica or incorporated into the silica network because these elements are known as additives of glass materials [18].

Fig. 2 shows the result of lactic acid formation from dihydroxyacetone using a variety of silica-supported metal oxides. The products detected were lactic acid (LA), pyruvaldehyde (PA) and glyceraldehyde (GLA). Among the silica-supported catalysts tested, the chromium oxide catalyst gave the highest yield of LA of 46% with a high conversion of dihydroxyacetone of 72% and a selectivity to LA of 64%. The titanium oxide catalyst gave a moderate yield of LA of 29%, and the gallium oxide catalyst of 27%. The titanium oxide catalyst also afforded an intermediate, PA with high selectivity of 43%. The lead oxide catalyst gave undetected products likely due to polymerization. Other metal oxides such as Mn, Zn, and W oxides showed high conversion, but no or little yields of LA. After the reaction using these unselective catalysts, the solutions were colored dark brown, which is indicative of deep polymerization. Table 1 summarizes the results of crystal structure, surface area, and the catalytic activity of a variety of silica-supported

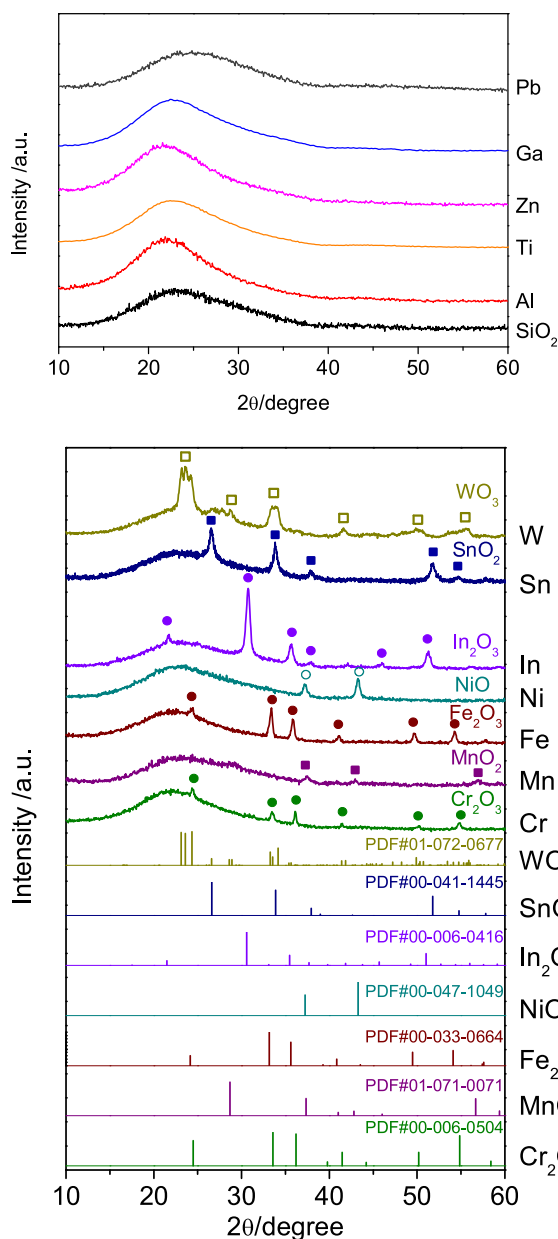


Fig. 1. XRD patterns of silica-supported metal oxide catalysts.

metal oxide catalysts. All silica-supported metal oxides showed lower BET surface areas than the silica support. The samples of amorphous oxides such as Pb, Ga and Zn had much lower surface areas, indicating that these metal species were incorporated into the silica network. There was no correlation between the surface area and conversion of DHA. From these results, the catalytic activity and textural properties of silica-supported chromium oxide and titanium oxide catalysts were further investigated.

### 3.2. Silica-supported titanium oxide and chromium oxide catalysts

Fig. 3 shows the time course of transformation of dihydroxyacetone using silica-supported titanium oxide and chromium oxide catalysts. In the initial stage of the reaction, GLA and PA were formed. With increase of reaction time, yields of these intermediates decreased, and LA was successively formed as a final product. The titanium oxide catalyst exhibited a higher conversion rate of DHA with a higher concentration of PA than the chromium oxide catalyst. However, the titanium oxide showed a lower consumption rate of PA and lower formation rate of LA

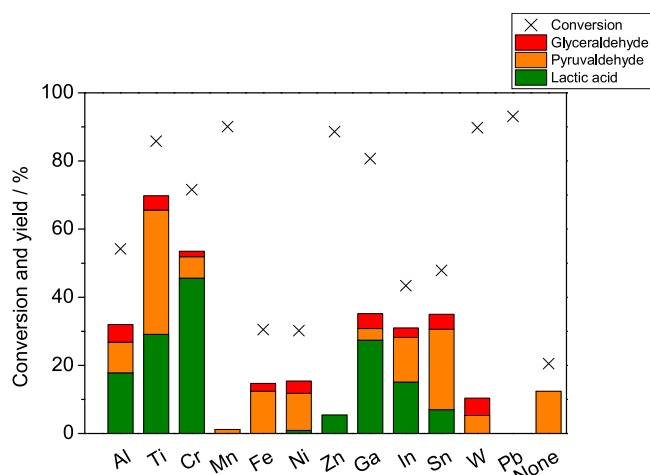


Fig. 2. Dihydroxyacetone conversion using a variety of silica-supported metal oxide catalysts. Reaction conditions: Dihydroxyacetone (0.55 mmol), catalyst (50 mg, metal loading; 1 mmol/g-support), water (3 mL), 130 °C, 3 h.

Table 1

Transformation of DHA using a variety of silica-supported metal oxide catalysts<sup>a</sup>.

Catalyst	Crystal phase	$S_{\text{BET}}/\text{m}^2\text{g}^{-1}$	Conv. /%	Selectivity /%		
				GLA	PA	LA
Al(1.0)/SiO <sub>2</sub>	Amorphous	273	54	10	17	33
Ti(1.0)/SiO <sub>2</sub>	Amorphous	292	86	5	43	34
Cr(1.0)/SiO <sub>2</sub>	Cr <sub>2</sub> O <sub>3</sub>	280	72	2	9	64
Mn(1.0)/SiO <sub>2</sub>	MnO <sub>2</sub>	314	90	0	1	0
Fe(1.0)/SiO <sub>2</sub>	Fe <sub>2</sub> O <sub>3</sub>	306	31	8	41	0
Ni(1.0)/SiO <sub>2</sub>	NiO	318	30	12	36	3
Zn(1.0)/SiO <sub>2</sub>	Amorphous	265	89	0	0	6
Ga(1.0)/SiO <sub>2</sub>	Amorphous	237	81	5	4	34
In(1.0)/SiO <sub>2</sub>	In <sub>2</sub> O <sub>3</sub>	265	43	6	30	35
Sn(1.0)/SiO <sub>2</sub>	SnO <sub>2</sub>	304	48	9	49	15
W(1.0)/SiO <sub>2</sub>	WO <sub>3</sub>	270	90	6	6	0
Pb(1.0)/SiO <sub>2</sub>	Amorphous	186	93	0	0	0
SiO <sub>2</sub>		323	21	0	60	0

<sup>a</sup> Reaction conditions: Dihydroxyacetone (0.55 mmol), catalyst (50 mg, metal loading; 1 mmol/g-support), water (3 mL), 130 °C, 3 h.

than the chromium oxide, resulting in a moderate yield of LA.

In contrast, the chromium oxide catalyst showed a lower conversion rate of DHA than the titanium oxide but afforded higher selectivity to LA. At ca. 50% conversion, the selectivity to LA was 46% for the chromium oxide catalyst (2 h reaction), compared to 18% for the titanium oxide catalyst (0.5 h reaction). After 9 h, the chromium oxide catalyst showed a high LA selectivity of 68% at a conversion of 95%. The titanium oxide catalyst afforded an LA selectivity of 47% at full conversion. These results indicated that the titanium oxide catalyst could quickly convert DHA to PA, and the chromium oxide catalyst could smoothly transform PA to LA. Therefore, the nature of the active sites was deduced to be different between these two catalysts.

Solid acid properties of silica-supported titanium oxide and chromium oxide were evaluated by using FTIR of adsorbed pyridine. The results are shown in Fig. 4. Two characteristic peaks attributed to Brønsted acid sites (ca. 1545 cm<sup>-1</sup>) and Lewis acid sites (ca. 1455 cm<sup>-1</sup>) were observed for both samples. For Ti(1.0)/SiO<sub>2</sub>, the amount of Brønsted acid sites was 0.32 mmol g<sup>-1</sup>, and those of Lewis acid sites was 0.24 mmol g<sup>-1</sup> with the low ratio of Lewis/Brønsted acid being 0.75. For Cr(1.0)/SiO<sub>2</sub>, the amount of Brønsted acid sites was 0.16 mmol g<sup>-1</sup>, and that of Lewis acid sites was 0.48 mmol g<sup>-1</sup>. The ratio of Lewis acid sites to Brønsted acid sites was 3. Although both samples had both Brønsted acid sites and Lewis acid sites, the titanium

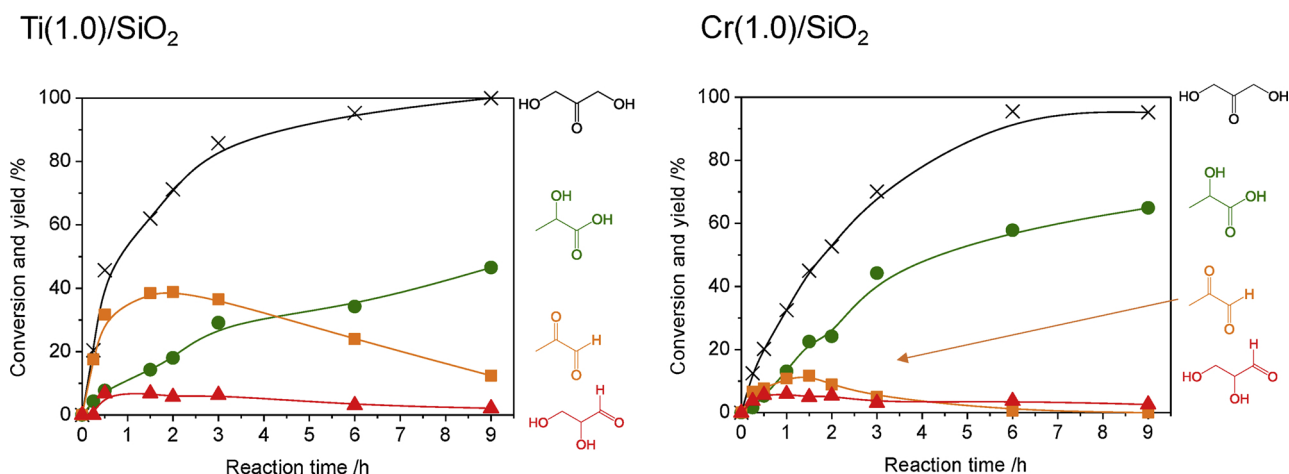


Fig. 3. Time course of dihydroxyacetone transformation using silica-supported titanium oxide catalyst and silica-supported chromium oxide catalyst. Reaction conditions: Dihydroxyacetone (0.55 mmol), catalyst (50 mg, metal loading; 1 mmol/g-support), water (3 mL), 130 °C.

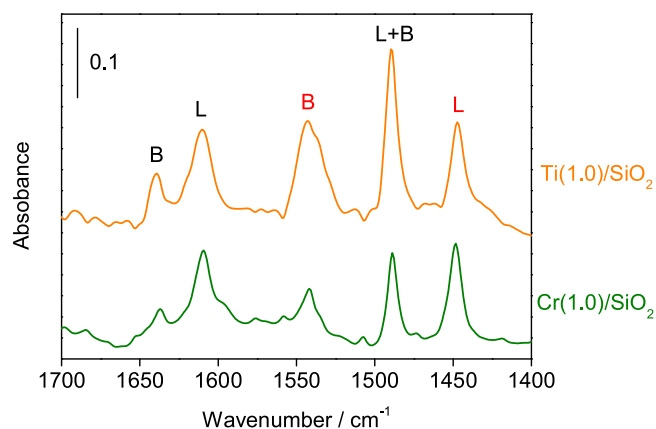


Fig. 4. Pyridine-adsorbed FTIR spectra for silica-supported chromium oxide and silica-supported titanium oxide. Self-supporting disk of 30 mg. 100 °C.

oxide catalyst had more Brønsted acid sites, and the chromium oxide catalyst had more Lewis acid sites. This difference could explain the reason for the contrast in the reaction results.

### 3.3. Effect of loading amount of titanium oxide and chromium oxide

The two metal oxide catalysts were further studied. The effect of loading amount on the state of impregnated metal species and their activities was investigated.

Fig. 5 shows XRD patterns of Ti(0.5)/SiO<sub>2</sub>, Ti(1.0)/SiO<sub>2</sub>, and Ti(2.0)/SiO<sub>2</sub> catalysts. No apparent peaks were observed for all samples, indicating no formation of crystalline titanium oxide such as anatase.

Fig. 6 shows DR UV–vis spectra of Ti(0.5)/SiO<sub>2</sub>, Ti(1.0)/SiO<sub>2</sub>, and Ti(2.0)/SiO<sub>2</sub> catalysts. A band centered at 200 nm was observed for Ti(0.5)/SiO<sub>2</sub> and Ti(1.0)/SiO<sub>2</sub> samples, which was attributed to tetrahedral titanium species. Additionally, broad bands centered at 250 nm and 300 nm were seen for both samples, which were assigned to octahedral titanium species and [TiO<sub>2</sub>]<sub>n</sub> clusters, respectively [19,20]. A band centered at 330 nm, corresponding to anatase TiO<sub>2</sub> was not observed, in good agreement with the XRD patterns [21]. A sharp band centered at 200 nm was not observed for Ti(2.0)/SiO<sub>2</sub>, suggesting that most of the titanium species were in octahedral coordination.

Table 2 shows the results of the transformation of DHA over Ti/SiO<sub>2</sub>. Here, the molar ratio of DHA to metal was set as 11.1 by varying the weight of catalyst used. With increase of the loading amount of titanium oxide, the conversion of DHA decreased. To achieve ca. 50% conversion, Ti(0.5)/SiO<sub>2</sub> required 0.5 h whereas Ti(2.0)/SiO<sub>2</sub> needed

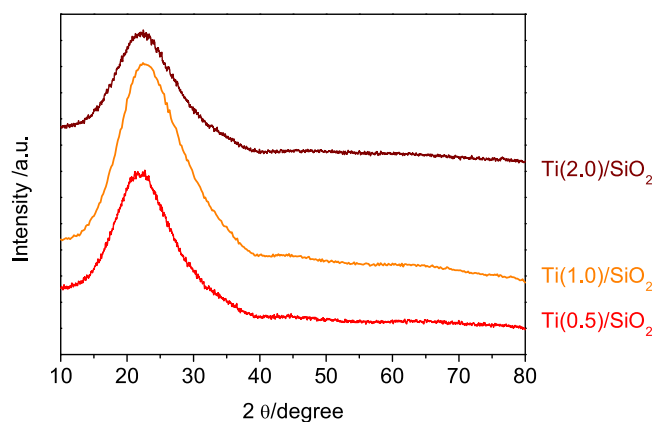


Fig. 5. XRD patterns of silica-supported titanium oxide catalysts.

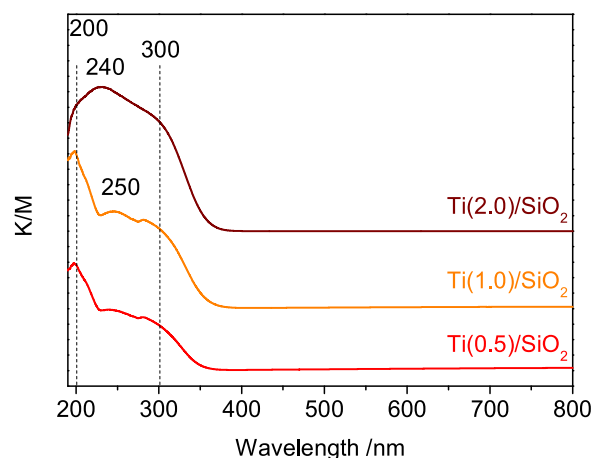


Fig. 6. DR UV–vis spectra of silica-supported titanium oxide catalysts.

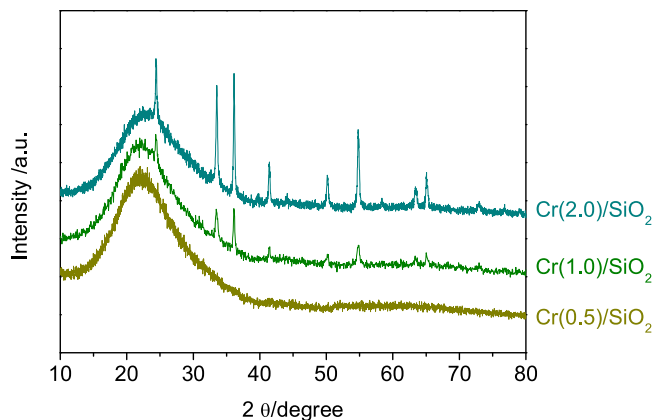
1.5 h. At the same conversion, the product selectivity was nearly the same with all the samples giving a high amount of PA. Table 2 also lists the number of Brønsted acid and Lewis acid sites on the catalysts used for the reaction. The number of Brønsted acid sites decreased with the increase in loading amount. This trend was consistent with the decrease in the conversion, suggesting that Brønsted acid sites mostly catalyzed the conversion of DHA to PA on titanium oxide.

Fig. 7 shows XRD patterns of Cr(0.5)/SiO<sub>2</sub>, Cr(1.0)/SiO<sub>2</sub>, and Cr(2.0)/SiO<sub>2</sub> catalysts. A clear difference among samples was observed.

**Table 2**  
DHA transformation over silica-supported titanium oxide catalysts <sup>a</sup>.

Catalyst	Amount of catalyst used /mg	Brønsted acid / $\mu\text{mol g}^{-1}$	Lewis acid / $\mu\text{mol g}^{-1}$	Reaction time /h	Conv. /%	Selectivity /%		
						GLA	PA	LA
Ti(0.5)/SiO <sub>2</sub>	100	140	110	0.5	52	12	69	19
Ti(1.0)/SiO <sub>2</sub>	50	240	320	0.5	46	15	75	18
				1.5	62	11	62	23
Ti(2.0)/SiO <sub>2</sub>	25	80	120	1.5	55	9	74	17

<sup>a</sup> Reaction conditions: Dihydroxyacetone (0.55 mmol), catalyst (25–100 mg, DHA/metal = 11.1), water (3 mL), 130 °C, 0.5 or 1.5 h.



**Fig. 7.** XRD patterns of silica-supported chromium oxide catalysts.

The samples of high loading amount, Cr(1.0)/SiO<sub>2</sub> and Cr(2.0)/SiO<sub>2</sub> had several peaks which could be assigned to a Cr<sub>2</sub>O<sub>3</sub> crystal phase. In contrast, Cr(0.5)/SiO<sub>2</sub> showed no peaks, indicating that chromium was highly dispersed on the silica support.

**Fig. 8** shows DR UV–vis spectra of silica-supported chromium oxide catalysts. Two distinct bands centered at 270 and 380 nm with a shoulder around 465 nm were observed for Cr(0.5)/SiO<sub>2</sub>. These bands were attributed to monochromate species in tetrahedral coordination [22,23]. The additional band centered at 465 nm was ascribed to polychromate species. At loadings higher than 1.0 mmol/g, a minor band at approximately 600 nm appeared. The band was assignable to crystalline chromium oxide,  $\alpha$ -Cr<sub>2</sub>O<sub>3</sub>, which was consistent with the XRD results.

**Table 3** summarizes the results of DHA transformation over the silica-supported chromium oxide catalysts. All samples gave high selectivity to LA, ca. 50%, which was distinctly different from the supported titanium oxide catalysts. The sample of Cr(1.0)/SiO<sub>2</sub> had the highest

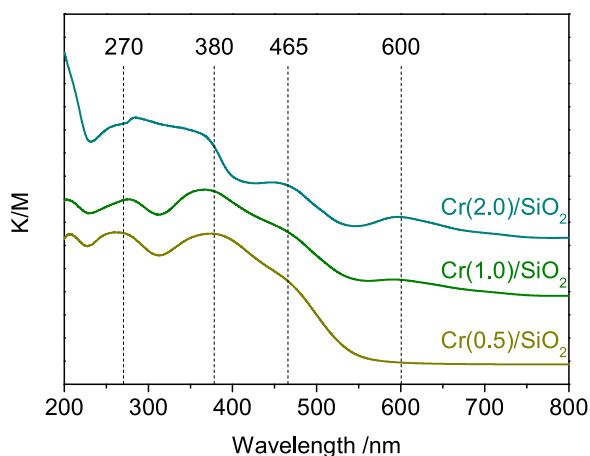


**Fig. 8.** DR UV–vis spectra of silica-supported chromium oxide catalysts.

amount of Lewis acid sites with the highest Lewis/Brønsted ratio, and afforded high selectivity to LA with the highest selectivity to PA. The sample of Cr(2.0)/SiO<sub>2</sub> also showed high selectivity to LA even at low conversion. With increase of the loading amount of Cr, the rate of DHA conversion decreased.

#### 3.4. Co-impregnation of chromium oxide and titanium oxide

It was found that the supported titanium oxide catalyst could quickly convert DHA to PA, and the chromium oxide catalyst could smoothly transform PA to LA. Thus, chromium and titanium were co-impregnated into silica support to combine their properties. **Fig. 9** shows DR UV–vis spectra for the silica-supported co-impregnated oxide catalysts. Two bands at 285 and 385 nm which were ascribed to monochromate species in tetrahedral coordination were observed for all catalysts. A band centered at ca. 200 nm attributed to tetrahedral titanium species was also observed.

**Table 4** shows amounts of Brønsted and Lewis acid sites of silica-supported co-impregnated oxide catalysts. **Fig. 10** shows the results of DHA transformation over the silica-supported co-impregnated oxide catalysts. The increase of Cr contents in the co-impregnated oxide catalysts increased both conversion of DHA and selectivity to LA with a decrease of selectivity to PA and GLA. The Cr(0.5)-Ti(0.5)/SiO<sub>2</sub> catalyst gave the highest selectivity to LA (84%) at a conversion of 85% for 1.5 h of reaction. Further increase of Cr content decreased both conversion and selectivity to LA. **Fig. 10** also plots the Lewis acid/Brønsted acid ratio as a function of Cr content. The co-impregnated catalysts showed high L/B ratio from 3.4 to 4.0. The trend of the L/B ratio was close to that of selectivity to lactic acid. The Cr(0.25)-Ti(0.75)/SiO<sub>2</sub> and Cr(0.5)-Ti(0.5)/SiO<sub>2</sub> catalysts had high L/B ratio which gave high selectivity to lactic acid at high DHA conversion.

**Fig. 11** shows the time course of transformation of DHA using the Cr(0.5)-Ti(0.5)/SiO<sub>2</sub> catalyst. As a comparison, a physical mixture of Cr(0.5)/SiO<sub>2</sub> and Ti(0.5)/SiO<sub>2</sub> was used. The co-impregnated catalyst, Cr(0.5)-Ti(0.5)/SiO<sub>2</sub> exhibited higher conversion with higher selectivity to LA than a physical mixture, Cr(0.5)/SiO<sub>2</sub> + Ti(0.5)/SiO<sub>2</sub>. The conversion reached almost 100% at 5 h with a high selectivity (or yield) to LA of 80%, which was the highest yield in this study. Although the physical mixture also showed high conversion and selectivity to LA, the selectivity to LA at full conversion was 72%, which was lower than that of the co-impregnated catalyst.

#### 3.5. Kinetic analysis of DHA transformation using silica-supported chromium oxide, titanium oxide, and the co-impregnated oxide catalysts

A kinetic analysis assessed the reaction pathways to LA using the co-impregnated catalyst. **Fig. 12** shows the time course of DHA conversion and product selectivity using the Cr(1.0)/SiO<sub>2</sub> catalyst. In the case of DHA (**Fig. 12a**) both GLA and PA were primary products because their selectivity started high and decreased. LA was a final product because its selectivity increased steadily with time. In the case of GLA (**Fig. 12b**) DHA was a primary product because its selectivity started high and monotonically decreased. PA was a secondary product because its selectivity started low, kept a constant, and then decreased. LA was a final

**Table 3**  
DHA transformation over silica-supported chromium oxide catalysts<sup>a</sup>.

Catalyst	Amount of catalyst used /mg	Brønsted acid / $\mu\text{mol g}^{-1}$	Lewis acid / $\mu\text{mol g}^{-1}$	L/B ratio <sup>b</sup>	Conv. /%	Selectivity /%		
						GLA	PA	LA
Cr(0.5)/SiO <sub>2</sub>	100	70	180	2.6	53	9	18	51
Cr(1.0)/SiO <sub>2</sub>	50	160	480	3.0	45	11	26	50
Cr(2.0)/SiO <sub>2</sub>	25	480	800	1.7	28	9	22	47

<sup>a</sup> Reaction conditions: Dihydroxyacetone (0.55 mmol), catalyst (25–100 mg), DHA/metal = 11.1, water (3 mL), 130 °C, 1.5 h. <sup>b</sup> Lewis acid/Brønsted acid.

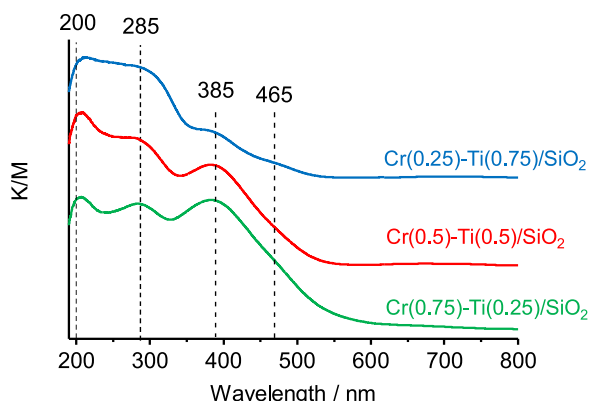


**Fig. 9.** DR UV-vis spectra of silica-supported co-impregnated chromium-titanium oxide catalysts.

**Table 4**  
Amounts of Brønsted and Lewis acid sites of silica-supported chromium-titanium mixed oxide catalysts<sup>a</sup>.

Catalyst	Brønsted acid / $\mu\text{mol g}^{-1}$	Lewis acid / $\mu\text{mol g}^{-1}$	L/B ratio <sup>a</sup>
Ti(1.0)/SiO <sub>2</sub>	240	320	1.3
Cr(0.25)-Ti(0.75)/SiO <sub>2</sub>	220	880	4.0
Cr(0.5)-Ti(0.5)/SiO <sub>2</sub>	100	400	3.8
Cr(0.75)-Ti(0.25)/SiO <sub>2</sub>	100	320	3.4
Cr(1.0)/SiO <sub>2</sub>	160	480	3.0
Cr(0.5)/SiO <sub>2</sub> + Ti(0.5)/SiO <sub>2</sub>	180	320	1.8

<sup>a</sup> Lewis acid/Brønsted acid.

product because its selectivity increased with time. From these results, the reaction pathway is proposed as shown in Scheme 2 [24]. The finding that GLA was a primary product from DHA and that conversely DHA was a primary product from GLA indicates that their inter-conversion is reversible. Other pathways are added for formation of undetected byproducts which were likely oligomers, the so-called humins.

Fig. 13 shows the time course of triose transformation using Cr(1.0)/SiO<sub>2</sub>, Ti(1.0)/SiO<sub>2</sub> and Cr(0.5)-Ti(0.5)/SiO<sub>2</sub> catalysts. The points are experimental results and the curves are calculated fits. Although the use of kinetic models such as Langmuir-Hinshelwood mechanism and rake mechanism [25] is desirable, for simplicity, the pseudo-first-order model was used. Calculations were conducted with Polymath 6.10 using the RKF 45 method to solve the following differential equations which were based on the literature [24].

$$\frac{d[DHA]}{dt} = -k_P[DHA] - k_G[DHA] + k_G^-[GLY] - k_{GO}[DHA][GLY]$$

$$\frac{d[GLY]}{dt} = k_G[DHA] - k_G^-[GLY] - k_{GO}[DHA][GLY]$$

$$\frac{d[PA]}{dt} = k_P[DHA] - k_L[PA] - k_{PO}[PA]^2$$

$$\frac{d[LA]}{dt} = k_L[PA]$$

$$\frac{d[\text{Oligomers}]}{dt} = k_{GO}[DHA][GLY] + k_{PO}[PA]^2$$

Table 5 lists the reaction rate constants used for the fitting. The constant  $k_P$  describes the conversion of DHA to PA, and the constant  $k_L$  the transformation of PA to LA. The constant  $k_G$  describes the

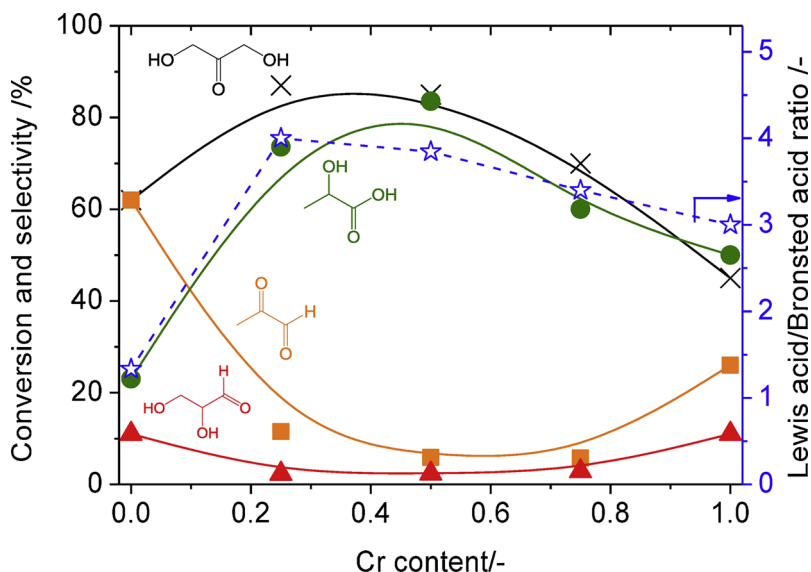


**Fig. 10.** Conversion of DHA, selectivity of products, and Lewis acid/Brønsted acid ratios as a function of chromium contents in silica-supported chromium-titanium mixed oxides. Reaction conditions: Dihydroxyacetone (0.55 mmol), catalyst (50 mg), water (3 mL), 130 °C, 1.5 h.

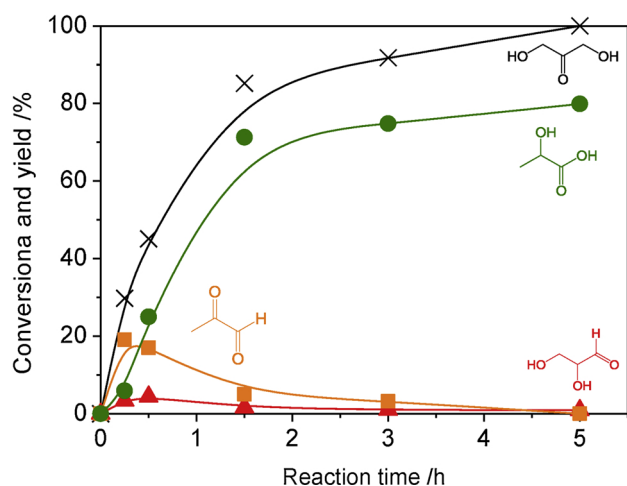
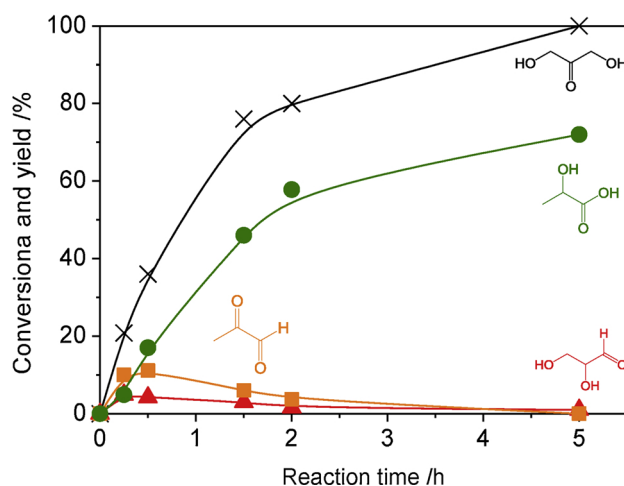
Cr(0.5)-Ti(0.5)/SiO<sub>2</sub>Cr(0.5)/SiO<sub>2</sub> + Ti(0.5)/SiO<sub>2</sub>  
Physical mixture

Fig. 11. Time course of dihydroxyacetone transformation using silica-supported chromium-titanium mixed oxide catalysts and a physical mixture of silica-supported chromium oxide and titanium oxide catalysts. Reaction conditions: Dihydroxyacetone (0.55 mmol), catalyst (50 mg), water (3 mL), 130 °C.

isomerization of DHA to GLA, and the constant  $k_G^-$  its back reaction. The constants  $k_{GO}$  and  $k_{PO}$  describe the formation of oligomers from GLA and PA, respectively. Good fits were obtained for all species.

It should be noted that the results of DHA and GLA transformation on Cr(1.0)/SiO<sub>2</sub> were well fitting using the same rate constants regardless of the reactants, which supports the accuracy of the proposed reaction pathway. The rate of DHA consumption for the Cr catalyst was moderate because the constant for formation of PA,  $k_p$  was small and the constant for the back reaction from GLA,  $k_G^-$  was considerably larger. The large constant for the back reaction was in good agreement with the result of the reaction using GLA as a reactant. In contrast, the rate of DHA consumption for the Ti catalyst was high because of the large rate constant for the formation of PA,  $k_p$  as well as the small influence of the isomerization between DHA and GLA. The constant for production of LA,  $k_L$  was small, resulting in lower selectivity to LA than the Cr catalyst.

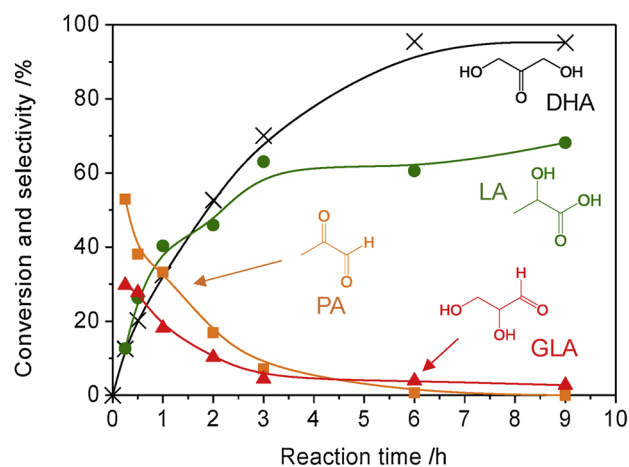
It is apparent that the combination of Cr and Ti was effective to increase the two critical constants,  $k_p$  and  $k_L$ , resulting in the higher

conversion rate with higher selectivity to LA. The constant of PA formation  $k_p$  for the Cr-Ti catalyst was three times larger than that for the Cr catalyst, and twice of that for the Ti catalyst. The constant of LA formation,  $k_L$  for the Cr-Ti catalyst was 1.7 times larger than that for the Cr catalyst and 12.5 times larger than that for the Ti catalyst.

#### 4. Conclusions

The silica-supported metal oxide catalysts were used for the transformation of DHA to LA. Silica-supported chromium oxide and titanium oxide were active for the reaction in water. The titanium oxide catalyst was selective to PA and the chromium oxide catalyst to LA. The Brønsted acid sites of the titanium oxide and the Lewis acid sites of the chromium oxide were attributed to the conversion of DHA to PA, and successive transformation to LA, respectively. Co-impregnated chromium- and titanium oxides on the silica support resulted in isolated chromium and titanium species in tetrahedral coordination and accelerated the reaction rate with improved the LA yield of up to 80%.

#### a) DHA



#### b) GLA

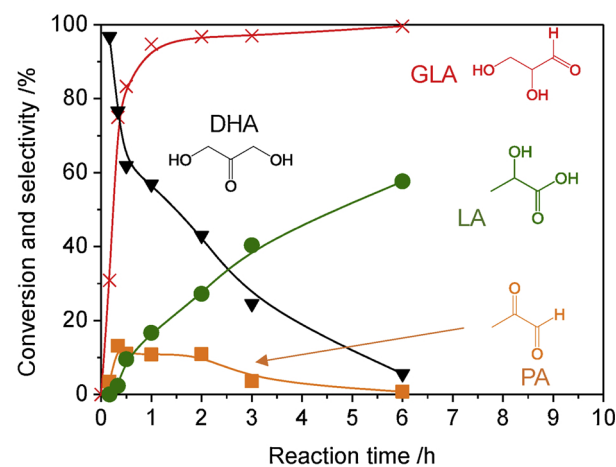
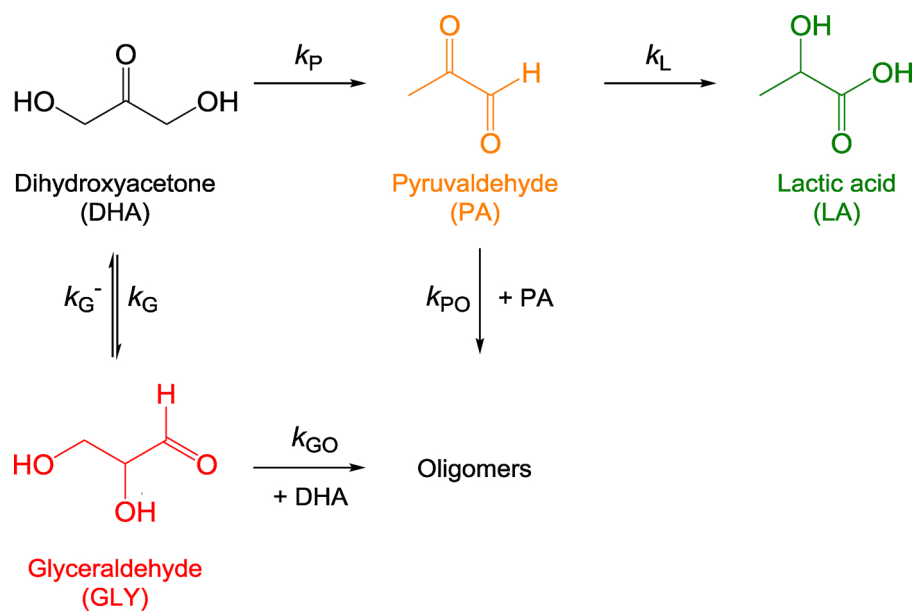
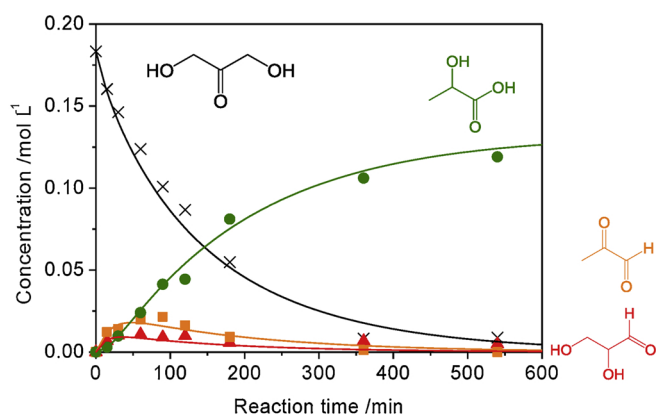


Fig. 12. Time course of dihydroxyacetone and glyceraldehyde transformation using silica-supported chromium oxide catalyst. Reaction conditions: a) Dihydroxyacetone or b) glyceraldehyde (0.55 mmol), catalyst (50 mg), water (3 mL), 130 °C. Conversions are indicated by ×.

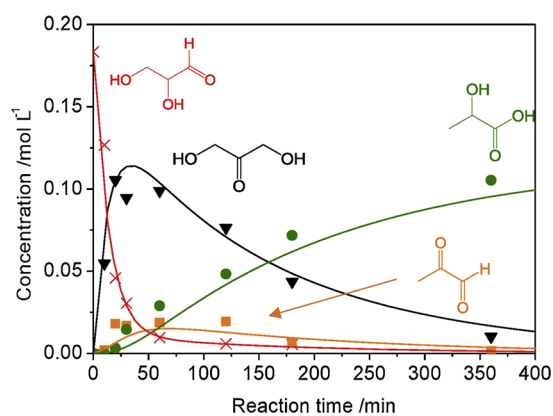


Scheme 2. Proposed reaction pathway for dihydroxyacetone transformation.

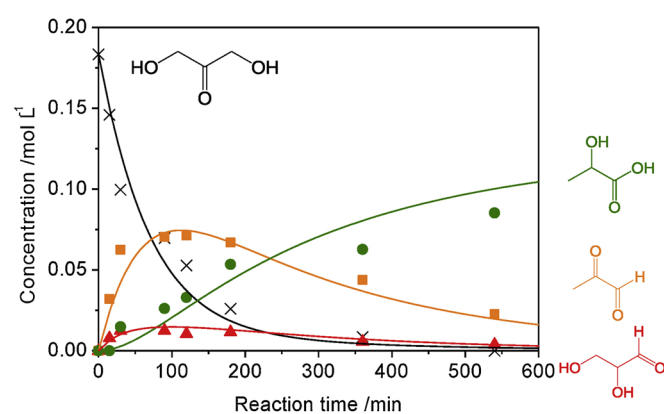
Cr(1.0) DHA



Cr(1.0) GLA



Ti(1.0)



Cr(0.5)-Ti(0.5)

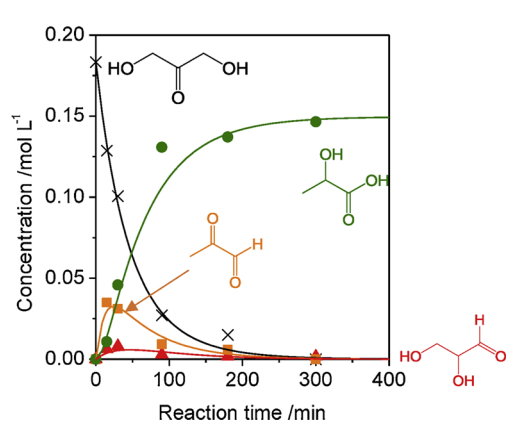


Fig. 13. Time course of triose transformation using Cr(1.0)/SiO<sub>2</sub>, Ti(1.0)/SiO<sub>2</sub> and Cr(0.5)-Ti(0.5)/SiO<sub>2</sub> catalysts. Reaction conditions: Dihydroxyacetone or glyceraldehyde (0.55 mmol), catalyst (50 mg), water (3 mL), 130 °C. The points are experimental results and the curves are calculated fits.

**Table 5**

Rate constants for DHA transformation using silica-supported chromium oxide, titanium oxide, and chromium-titanium oxide catalysts (units in  $\text{h}^{-1}$ ).

	$k_p$	$k_L$	$k_G$	$k_G^-$	$k_{GO}$	$k_{PO}$
Cr(1.0)/SiO <sub>2</sub>	0.36	1.8	0.3	3.8	4.8	36
Ti(1.0)/SiO <sub>2</sub>	0.6	0.24	0.18	1.1	6	1.2
Cr(0.5)-Ti(0.5)/SiO <sub>2</sub>	1.2	3	0.12	1.2	3	30

Kinetic analysis revealed that the rate constant for PA formation for the co-impregnated catalyst was 2–3 times higher and that of LA formation was 1.7–12.5 times higher than those for the Cr catalyst and the Ti catalyst.

### Acknowledgments

The authors thank Dr. Takayuki Iida for the UV-vis measurement. This work was supported by JSPS KAKENHI Grant Number JP 25709077.

### References

- [1] P. Mäki-Arvela, I.L. Simakova, T. Salmi, D.Y. Murzin, *Chem. Rev.* 114 (2014) 1909–1971.
- [2] M.S. Holm, S. Saravanamurugan, E. Taarning, *Science* 328 (2010) 602–605.
- [3] N. Razali, A.Z. Abdullah, *Appl. Catal. A Gen.* 543 (2017) 234–246.
- [4] L. Li, C. Stroobants, K. Lin, P.A. Jacobs, B.F. Sels, P.P. Pescarmona, *Green Chem.* 13 (2011) 1175–1181.
- [5] Y. Hayashi, Y. Sasaki, *Chem. Commun.* (2005) 2716–2718.
- [6] C.B. Rasrendra, B.A. Fachri, I.G.B.N. Makertihartha, S. Adisasmito, H.J. Heeres, *ChemSusChem* 4 (2011) 768–777.
- [7] R.M. West, M.S. Holm, S. Saravanamurugan, J. Xiong, Z. Beversdorf, E. Taarning, C.H. Christensen, *J. Catal.* 269 (2010) 122–130.
- [8] P.Y. Dapsens, C. Mondelli, J.P. Ramirez, *ChemSusChem* 6 (2013) 831–839.
- [9] P.Y. Dapsens, M.J. Menart, C. Mondelli, J.P. Ramirez, *Green Chem.* 16 (2014) 589–593.
- [10] Q. Guo, F. Fan, E.A. Pidko, W.N.P.V. van der Graaff, Z. Feng, C. Li, E.J.M. Hensen, *ChemSusChem* 6 (2013) 1352–1356.
- [11] L. Wang, J. Zhang, X. Wang, B. Zhang, W. Ji, X. Meng, J. Li, D.S. Su, X. Bao, F.-S. Xiao, *J. Mater. Chem. A* 2 (2014) 3725–3729.
- [12] F. de Clippel, M. Dusselier, R. van Rompaey, P. Vanelderer, J. Dijkmans, E. Makshina, L. Giebeler, S. Oswald, G.V. Baron, J.F.M. Denayer, P.P. Pescarmona, P.A. Jacobs, B.F. Sels, *J. Am. Chem. Soc.* 134 (2012) 10089–10101.
- [13] X. Wang, F. Liang, C. Huang, Y. Li, B. Chen, *Catal. Sci. Technol.* 5 (2015) 4410–4421.
- [14] X. Wang, F. Liang, C. Huang, Y. Li, B. Chen, *Catal. Sci. Technol.* 6 (2016) 6551–6560.
- [15] K. Nakajima, J. Hirata, M. Kim, N.K. Gupta, T. Murayama, A. Yoshida, N. Hiyoshi, A. Fukuoka, W. Ueda, *ACS Catal.* 8 (2018) 283–290.
- [16] C.A. Emeis, *J. Catal.* 141 (1993) 347–354.
- [17] Y. Wang, W. Deng, B. Wang, Q. Zhang, X. Wan, Z. Tang, Y. Wang, C. Zhu, Z. Cao, G. Wang, H. Wan, *Nat. Commun.* 4 (2013) 2141.
- [18] A.K. Yadav, P. Singh, *RSC Adv.* 5 (2015) 67583–67609.
- [19] S. Sakugawa, K. Wada, M. Inoue, *J. Catal.* 275 (2010) 280–287.
- [20] T.A. Zepedaa, A.I. Molina, J.N.D. Leon, R.O. Estrella, S. Fuentes, G.A. Nunez, B. Pawelec, *J. Mol. Catal. A Chem.* 397 (2015) 26–35.
- [21] K.-M. Choi, T. Yokoi, T. Tatsumi, K. Kuroda, *J. Mater. Chem. A* 1 (2013) 2485–2494.
- [22] Y. Wang, Y. Ohnishi, T. Shishido, Q. Zhang, W. Yang, Q. Guo, H. Wan, K. Takehira, *J. Catal.* 220 (2003) 347–357.
- [23] S. Dzwigaj, T. Shishido, *J. Phys. Chem. C* 112 (2008) 5803–5809.
- [24] D. Jolimaire, D. Delcroix, N. Essayem, C. Pinel, M. Besson, *Catal. Sci. Technol.* 8 (2018) 1349–1356.
- [25] A. Cho, H. Kim, A. Iino, A. Takagaki, S.T. Oyama, *J. Catal.* 318 (2014) 151–161.